Redox Properties of Plant Biomass-Derived Black Carbon (Biochar)

2

Redox properties of plant biomass-derived black carbon (biochar)

4

5   Laura Klüpfel[†], Marco Keiluweit[§,‡], Markus Kleber[§,¶], and Michael Sander[†,*]

6

7   [†] Department of Environmental Systems Sciences
8   Institute of Biogeochemistry and Pollutant Dynamics
9   Swiss Federal Institute of Technology (ETH) Zurich, 8092 Zurich, Switzerland
10
11   § Department of Crop and Soil Science
12   Soil and Environmental Geochemistry
13   Oregon State University, Corvallis, OR 97331, United States
14   ¶ Institute of Soil Landscape Research, Leibniz-Center for Agricultural Landscape
15   Research (ZALF), 15374 Müncheberg, Germany
16
17   [‡] Department of Environmental Earth System Science
18   Soil and Environmental Biogeochemistry
19   Stanford University, Stanford, CA 94305, USA
20

21

24

25

26   *To whom correspondence should be addressed.
27   E-mail: michael.sander@env.ethz.ch
28   Phone: +41-(0)44 6328314
29   Fax: +41 (0)44 633 1122

30

31   Number of pages: 30

32   Number of figures: 4

33   Number of tables: 1

34   Number of words: 7261
35   (=5161+ 300 Table 1 + 600 Figure 1 + 600 Figure 2 + 300
36   Figure 3 + 300 Figure 4)

37

38   **Abstract**

39   Soils and sediments worldwide contain appreciable amounts of thermally altered

40   organic matter (chars) of both natural and industrial origin. Additions of chars into

41   soils are discussed as a strategy to mitigate climate change. Chars contain

42   electroactive quinoid functional groups and polycondensed aromatic sheets that were

43   recently shown to be of biogeochemical and enviro-technical relevance. However, so

44   far no systematic investigation of the redox properties of chars formed under different

45   pyrolysis conditions has been performed. Here, using mediated electrochemical

46   analysis, we show that chars made from different feedstock and over a range of

47   pyrolysis conditions are redox-active and reversibly accept and donate up to 2 mmol

48   electrons per gram of char. The analysis of two thermosequences revealed that chars

49   produced at intermediate to high heat treatment temperatures (HTTs) (400-700°C)

50   show the highest capacities to accept and donate electrons. The electron accepting

51   capacities (EACs) increase with the nominal carbon oxidation state of the chars.

52   Comparable trends of EACs and of quinoid C=O contents with HTT suggest quinoid

53   moieties as major electron acceptors in the chars. We propose to consider chars in

54   environmental engineering applications that require controlled electron transfer

55   reactions. Electroactive char components may also contribute to the redox properties

56   of traditionally defined "humic substances".

57

58   **Introduction**

59   Char black carbon is formed by incomplete combustion of biomass and is

60   ubiquitous in the environment.[1-6] Chars make up significant fractions of the organic

61   matter in many soils and sediments.[7,8] By contributing to the slow cycling carbon

62   pool in these systems, chars link into the global carbon cycle.[3,9-11] In addition to their

2

63 biogeochemical relevance, chars also play a role in environmental engineering as

64 high affinity sorbents for organic and inorganic pollutants.[12-20] Sorption to chars

65 strongly affects the transport and bioavailability of xenobiota in natural systems, and

66 char amendments are considered as effective means to immobilize contaminants.[21-23]

67 An increasingly discussed aspect of char functionality is their apparent role as

68 electron transfer catalysts in redox reactions of both biogeochemical and enviro-

69 technical relevance.[24,25] Chars catalyze the reductive transformation of organic

70 contaminants by facilitating electron transfer from bulk chemical electron donors to

71 the receiving organic compounds.[26-32] Electron shuttling towards denitrifying

72 microorganisms in soils was invoked to rationalize lower N_2O emissions from char

73 amended soils compared to non-amended control treatments.[33-35]

74   Electron transfer catalysis by intermediate and high temperature chars may involve

75 two types of redox-active structures: quinone-hydroquinone moieties and/or

76 conjugated π-electron systems associated with condensed aromatic (sub-) structures

77 of the char.[26,27,32] The presence of quinone moieties is directly supported by evidence

78 from carbon Near-Edge X-ray Absorption Fine Structure Spectroscopy

79 (NEXAFS)[36,37] and from electron paramagnetic resonance spectroscopy,[38] which

80 suggests that certain chars contain radicals of semiquinone-type character. These

81 spectroscopic analyses find highest quinone concentrations in intermediate to high

82 temperature chars. The alleged importance of quinone/hydroquinone pairs as electron

83 accepting and donating moieties in chars is supported by the fact that these moieties

84 are major contributors to the redox properties and reactivities of other types of

85 organic matter and carbonaceous solids, including dissolved organic matter,[39-42]

86 particulate organic matter,[43,44] activated carbons and carbon black.[45-49] In addition to

87 quinone/hydroquinone moieties, the condensed aromatic (sub-) structures of chars

88 may be electroactive by allowing electrons to be transferred across the conjugated

89 π−electron systems. Electron conductance in and electron transfer to and from such

90 systems is well established for graphite, carbon nanotubes,[50,51] fullerenes,[52,53] and

91 graphene oxide.[54,55] The extent of aromatic ring condensation and hence the ratio of

92 sp^2 to sp^3 hybridized carbons in chars increases with increasing charring

93 temperature.[36,56-59] At heat treatment temperatures (HTTs) above 600°C, conjugated

94 aromatic sheets grow sufficiently large for chars to achieve conductivity.[25,32,60]

95 However, while an increase in HTT increases aromaticity and the extent of ring

96 condensation, it concomitantly decreases the char oxygen content and yield.[36,58]

97 Based on these opposing trends, it is reasonable to expect that the contribution of

98 quinone/hydroquinone moieties to the electron transfer properties of chars would

99 decrease with increasing HTT while the contribution of conjugated π−electron

100 systems should increase with HTT.

101   The presence of redox-active moieties in chars and the growing evidence that

102 chars are important electron transfer catalysts in biogeochemical and pollutant redox

103 reactions calls for a systematic assessment of the redox properties of chars. Up to

104 now, such a systematic investigation has been hampered by the lack of an appropriate

105 experimental technique. Traditional approaches to characterize the redox properties

106 of dissolved and particulate natural organic matter rely on measuring the reduction of

107 a chemical oxidant, typically complexed Fe^{3+} species or iodine.[61-64] Among these

108 approaches is the ferric reducing antioxidant power assay, which was recently used to

109 quantify the electron donating capacities of char water extracts.[65] Quantification of

110 electron transfer by these traditional approaches is, however, only indirect (i.e.,

111 conversion of the added oxidant Fe^{3+} or I_2), unidirectional (i.e., in the oxidative

112 direction but not in the reductive direction), and not conducted at a constant reduction

4

113   potential, E_h (i.e., the E_h decreases as the chemical oxidant is being reduced). These

114   shortcomings were recently overcome by mediated electrochemical analysis, a novel

115   analytical approach which allows for a direct and bidirectional quantification of

116   electron transfer to and from humic substances[40,41,66] and Fe-bearing mineral

117   phases[67-69] under constant and well-controlled redox conditions.

118   The goal of this study was to systematically assess how redox properties may vary

119   among a variety of char types. More specifically, we aimed at (i) validating the use of

120   mediated electrochemical analysis to characterize the redox properties of chars, (ii)

121   systematically quantifying the changes in the electron accepting and donating

122   capacities of chars formed under different pyrolysis conditions, including variations

123   in HTT and feedstock, and (iii) assessing the reversibility of electron transfer to

124   chars. To address these points, we quantified the electron accepting and donating

125   capacities of a total of 19 chars and investigated the reversibility of the electron

126   transfer to these chars. The chars examined included two thermosequences of six

127   temperature steps (200-700˚C) each from a grass and a wood feedstock as well as

128   seven reference chars.

129

130   **Experimental Section**

131   *Chemicals.* Acetic acid (puriss. p.a.), hypochloric acid (37%), potassium chloride

132   (puriss. p.a.), sodium borohydride (puriss. p.a.), and sodium hydroxide (32%) were

133   purchased from Fluka. Sodium phosphate dibasic (p.a.) and ubiquinone (Q_{10}) (>98%)

134   were from Sigma-Aldrich. The electron transfer mediator 2,2'-azino-bis(3-

135   ethylbenzothiazoline-6-sulfonic acid) diammonium salt (ABTS) (>99%) was from

136   Fluka and the zwitterionic viologen 4,4'-bipyridinium-1,1'-bis(2-ethylsulfonate)

137   (ZiV) was synthesized and purified as detailed elsewhere.[69]

138   *Solutions*. Nanopure water (resistivity, $\sigma > 18$ MΩ·cm) was used for all

139   experiments. All solutions prepared under oxic conditions were made anoxic by

140   purging with N_2 (1 h at 80 °C and 1 h at room temperature) prior to transfer into the

141   glovebox ($O_2 < 0.1$ ppm).

142   *Chars.* A total of 19 chars were analyzed. Two sets of six chars each were from a

143   grass (tall fescue, *Festuca arundinacea*) and a wood (ponderosa pine, *Pinus*

144   *ponderosa*) char thermosequence that was previously characterized[36] (abbreviated as

145   GX and WX, respectively, where X corresponds to HTTs ranging from 200 to

146   700°C). Five additional chars were produced in a semi-industrial retort following a

147   procedure described elsewhere[70] and included chars from hazelnut (HZ, *Corylus*

148   *avellana L. varietas 'Barcelona'*) shell/wood formed at 400, 550, and 700°C and

149   Douglas-fir (DF, *Pseudotsuga menziesii* at 400 and 700°C. Two reference chars[71-73]

150   from rice straw (*Oryza sativa* Arborio) and chestnut (*Castanea sativa*) wood

151   (abbreviated as RS and CW, respectively) were charred in a N_2-atmosphere at a HTT

152   of 450°C. Key physicochemical properties of the wood and grass thermosequence

153   chars are given in **Table 1** and of the other chars in **Table S1**.

154   *Preparation of char suspensions*. All chars were finely ground in Eppendorf tubes

155   using ball mills, as detailed in the Supporting Information (SI). The particle size

156   distributions of the pulverized chars are shown in **Figure S1**. The chars were placed

157   under vacuum in the antechamber of an anoxic glovebox over night to remove

158   adsorbed O_2, then transferred into the glovebox, and suspended in anoxic buffer

159   solution (pH 7, 0.1 M phosphate, 0.1 M KCl) in glass vials to final concentrations of

160   1 or 4 g char L^{-1}. The glass vials were crimp-capped with butyl rubber stoppers,

161   transferred out of the glovebox, and positioned in a water bath underneath an

162   ultrasonic tip (Sonics Vibra-cell VCX 500 with microtip, amplitude 150 W, 10 min)

163　to finely disperse the chars. The chars were transferred back into the glovebox for

164　electrochemical analysis.

165

166　**Table 1.** Elemental composition, nominal average carbon oxidation state (C_{ox}),
167　double bond equivalents (DBE), aromaticity index (AI), and C=O contents of the
168　grass (GX) and wood (WX) thermosequence chars, where X corresponds to the
169　charring temperature in °C.
170

Char specimen	Elemental composition [mmol element (g char)$^{-1}$][a]				Nominal C oxidation state C_{ox}[b]	DBE[c] [mol DBE (mol C)$^{-1}$]	AI[c] [mol DBE$_{AI}$ (mol C)$^{-1}$]	C=O[d] content [mmol C=O (g char)$^{-1}$]
	C	N	H	O				
G700	78.4	0.50	15.3	2.3	-0.14	0.92	0.92	0.80
G600	74.1	0.71	24.7	4.8	-0.20	0.85	0.85	1.66
G500	68.4	0.78	33.2	8.4	-0.24	0.78	0.75	2.60
G400	64.4	0.89	47.0	10.4	-0.40	0.66	0.60	2.79
G300	49.7	0.73	66.4	20.4	-0.50	0.36	0.00	2.33
G200	39.3	0.44	71.1	28.2	-0.36	0.13	0.00	0.25
W700	76.8	0.06	16.1	3.8	-0.11	0.91	0.90	1.2
W600	74.1	0.04	29.7	5.0	-0.27	0.81	0.80	1.7
W500	68.2	0.06	35.1	9.1	-0.25	0.76	0.72	2.8
W400	61.7	0.04	49.1	13.1	-0.37	0.62	0.52	3.1
W300	45.6	0.04	64.5	24.2	-0.35	0.32	0.00	1.7
W200	42.4	0.03	68.9	26.4	-0.38	0.21	0.00	-

171　[a] Elemental composition data from reference[36]. [b] Calculated according to reference[74]
172　[c] Calculated from elemental composition data according to reference[75]. [d] quinoid C=O content
173　based on NEXAFS spectra from reference[36].
174

175　***Q_{10} recovery experiment.*** Increasing amounts of apolar ubiquinone, Q_{10}, were

176　added from an ethanolic stock solution (0.94 ± 0.01 mM) to suspensions of G500 and

177　G400 chars (both at 1 g L^{-1}) to final concentrations between 0.19 and 0.53 mmol Q_{10}

178　(g G500)$^{-1}$ and between 0.19 and 0.76 mmol Q_{10} (g G400)$^{-1}$. The char suspensions

179　were stirred for 30 min to allow for Q_{10} sorption, followed by electrochemical

180　analysis. Extensive sorption of Q_{10} to the chars was verified by electrochemical

181　quantification of the dissolved Q_{10} in the supernatant of the char following

182　centrifugation of the samples, as detailed in the SI.

183　***Redox cycling of charcoals***. All chars were reduced with borohydride (NaBH$_4$)

184　and subsequently re-oxidized by O$_2$ in air. Changes in the char redox states were

185   determined by electrochemical analysis (see below) of untreated, NaBH$_4$-reduced,

186   and re-oxidized chars. Detailed descriptions of the borohydride reduction step and the

187   oxygen re-oxidation steps are provided in the SI.

188   *Electrochemical analysis*. The redox states of the chars were quantified by

189   mediated electrochemical reduction (MER) and oxidation (MEO), adapted from a

190   previously published method.[40] A nine mL glassy carbon cylinder (Sigradur G, HTW,

191   Germany) served both as the working electrode (WE) and electrochemical reaction

192   vessel. This WE setup significantly increased measurement sensitivity compared to

193   the original setup in which we used a vitreous carbon WE.[40] The applied redox

194   potentials E_h were measured against Ag/AgCl reference electrodes (Bioanalytical

195   Systems Inc., USA) but are reported with reference to the standard hydrogen

196   electrode. The counter electrode was a coiled platinum wire separated from the WE

197   compartment by a porous glass frit. The WE cylinder was filled with 6 mL buffer (0.1

198   M KCl, 0.1 M phosphate, pH 7) and equilibrated to the desired redox potential (E_h= -

199   0.49 V in MER and +0.61 V in MEO). Subsequently, 130 µL of stock solutions (10

200   mM) of the electron transfer mediators ZiV (in MER) or ABTS (in MEO) were added

201   to the cells, resulting in reductive and oxidative current peaks, respectively. After re-

202   attainment of constant background currents, small volumes (i.e., 20-100 µL) of the

203   char suspensions were spiked to the cells. The resulting reductive (MER) and

204   oxidative (MEO) current peaks were integrated to yield the electron accepting

205   capacities (EAC) and donating capacities (EDC) (both [mmol e$^-$ (g char)$^{-1}$]) of the

206   chars added:

207     $$EAC = \frac{\int \frac{I_{red}}{F} dt}{m_{char}}$$ **Eq. 1a**

208 $$EDC = \frac{\int \frac{I_{ox}}{F} dt}{m_{char}}$$ **Eq. 1b**

209 where I_{red} and I_{ox} (both [A]) are the baseline-corrected reductive and oxidative

210 currents in MER and MEO, respectively, F (=96485 [sec A/mol$_{e^-}$]) is the Faraday

211 constant, and m_{char} [g char] is the mass of added char. All char samples were analyzed

212 in at least duplicates (and most in triplicates) with t= 30 min between the analyses to

213 ensure baseline-separation of individual current peaks. The electron exchange

214 capacity (EEC= EAC + EDC) [mmol e$^-$ (g char)$^{-1}$] of a char describes its total

215 capacity to accept and donate electrons.

216
217 **Results and Discussion**

218 *Mediated electrochemical analysis of chars.* The applicability of mediated

219 electrochemical analysis to characterize the redox properties of chars was assessed by

220 analyzing four char specimen (G400, G500, W400, and W500) by MER and MEO.

221 **Figure 1a-d** shows the reductive and oxidative current peaks in MER and MEO,

222 respectively, that resulted from adding increasing amounts of the chars to the

223 electrochemical cells. Char masses smaller than 100 µg yielded strong current

224 responses, demonstrating the high sensitivity of MER and MEO. The high initial

225 reductive and oxidative currents following each char addition reflect high initial

226 electron transfer rates to and from the chars, respectively. The currents subsequently

227 decreased as the electron accepting and donating moieties in the chars approached

228 apparent E_h equilibrium (and hence no net electron transfer) with the E_h of the

229 mediators (= the E_h applied to the WEs). All chars showed well defined and base-line

230 separated current peaks, except for W500 with only small current responses in MEO

231 (panel a). Base-line separation implies that each char had come to apparent E_h-

232 equilibrium in the cells prior to addition of the next char sample. Electron transfer

233 kinetics to and from G400 and G500 were faster than to and from W400 and W500,

234 as evidenced by sharper current peaks of the former than the latter. Integration of the

235 current peaks yielded the numbers of electrons transferred to and from the chars, Q

236 [nmol e$^-$]. For all chars tested, Q was linearly proportional to the char mass analyzed

237 in both MER and MEO (**Figure 1a-d**, insets).

238   In addition to establishing linear responses of MER and MEO, we assessed the

239 extent to which MER and MEO quantified redox-active species on the char surfaces.

240 To this end, we sorbed increasing amounts of ubiquinone (Q_{10}) to the surfaces of

241 G500 and G400, followed by MER and MEO analysis. Sorption of the added Q_{10} to

242 G500 and G400 was extensive (adsorption of at least 92 % and 94 % of the added

243 Q_{10}, respectively), as detailed in the SI. **Figure 1e,f** shows that increasing amounts of

244 sorbed Q_{10} resulted in increasing EAC values of G400 and G500 that was in good

245 agreement with the expected increase based on a two-electron reduction of each Q_{10}

246 molecule. The EDC of G400 and G500 were not affected by Q_{10} sorption, consistent

247 with expectation since Q_{10} does not donate electrons. The lower than expected EAC

248 values measured at the highest sorbed Q_{10} concentrations likely resulted from an

249 ethanol co-solvent effect on the electrochemical measurement (i.e., the volumetric

250 contribution of ethanol to the char suspension was 44 % at the highest added Q_{10}

251 mass).
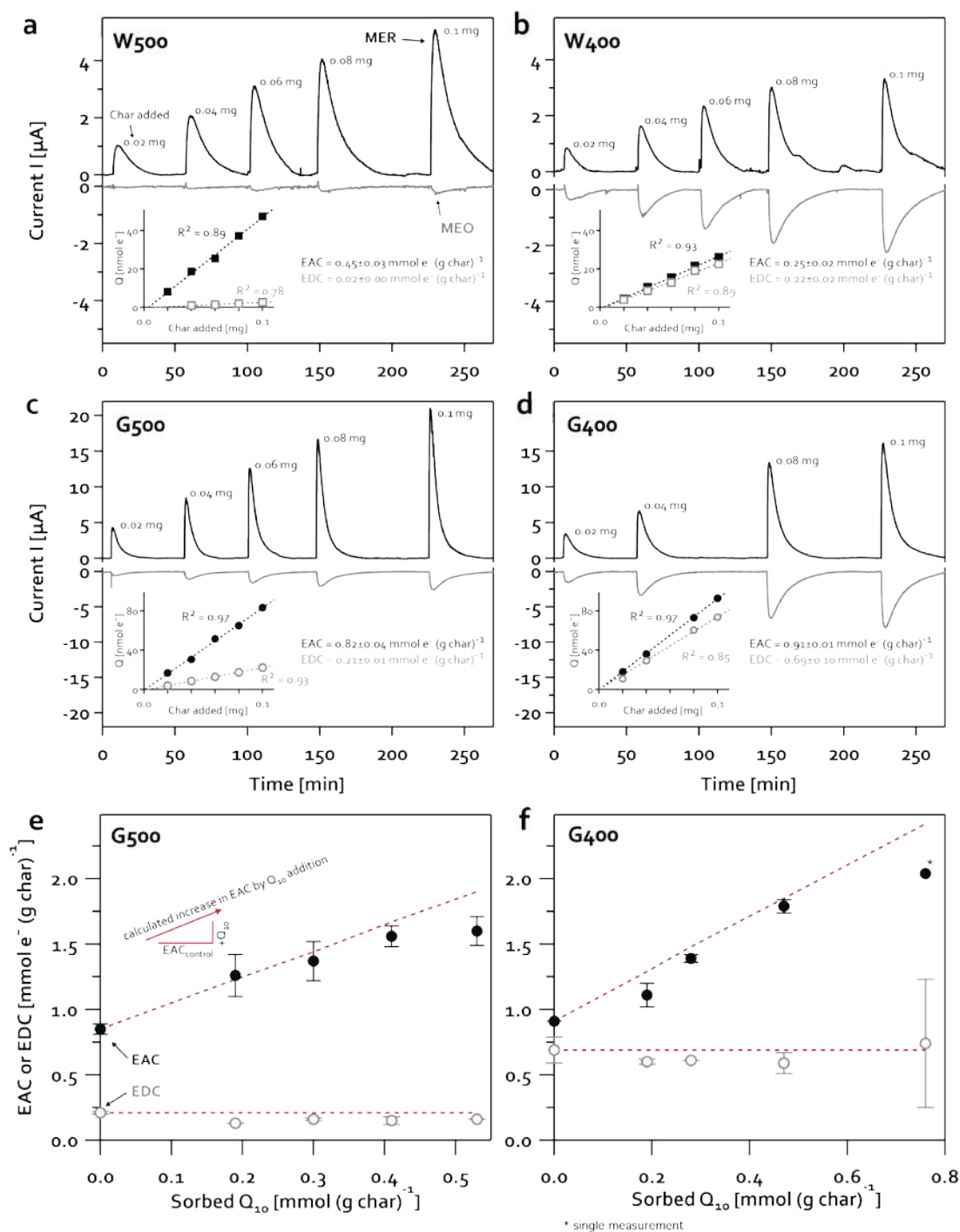
Figure 1 a-d. Reductive and oxidative current responses to increasing amounts of char specimen W400, W500, G400, and G500 analyzed by mediated electrochemical reduction (MER; E_h = -0.49 V, pH 7; black traces) and mediated electrochemical oxidation (MEO E_h= +0.61 V, pH 7; grey traces). The numbers above the current peaks denote the analyzed char masses. The numbers of electrons transferred to and from the chars, Q, increased linearly with increasing masses of char analyzed (inserts). The slopes of the linear regression lines of Q versus char mass correspond to the electron accepting and donating capacities (EAC and EDC; reported as averages ± standard deviation). **e,f.** EAC (black symbols) and EDC (grey symbols) values of G500 and G400 samples containing increasing adsorbed amounts of added

11

263 ubiquinone, Q_{10}. Error bars represent maximum and minimum values of duplicate
264 measurements. The asterisk in panel f indicates a single measurement. The red
265 dashed lines correspond to the EAC increase expected for the transfer of two
266 electrons per added Q_{10} molecule.
267
268   The high sensitivities and linear responses in Q to the analyzed char masses in

269 MER and MEO (**Figure 1a-d**), and the quantitative detection of exogenous Q_{10}

270 adsorbed to selected chars in MER (**Figure 1e,f**) demonstrated the applicability of

271 mediated electrochemical analysis to characterize the electron accepting and donating

272 properties of chars.

273   ***Effect of heat treatment temperature (HTT) on char redox properties.*** HTT is a

274 major factor that determines the physicochemical properties of chars.[76] We

275 systematically assessed the effect of HTT on char redox properties by quantifying the

276 EAC and EDC values for two thermosequences formed from grass and wood

277 feedstock. Only HTTs were varied in the formation of these chars, while all other

278 conditions were kept constant.[36]

279   **Figure 2a,b** shows that all tested grass and wood chars accepted and donated

280 electrons at the E_h applied in MER and MEO, respectively. At any given HTT above

281 200°C, the grass chars had higher absolute EAC (black symbols), EDC (grey

282 symbols), and EEC (horizontal black bars) values than the corresponding wood chars.

283 While there were differences in absolute capacities of grass and wood chars, the HTT

284 had comparable effects on the relative changes in the EAC, EDC, and EEC values for

285 both thermosequences. The EAC values were lowest for low-HTT chars (i.e., 200 and

286 300°C), highest for intermediate-HTT chars (i.e., 400 and 500°C; with maxima of

287 EAC= 0.90 mmol e⁻/g for G400 and 0.54 mmol e⁻/g for W500), and intermediate in

288 high-HTT chars (i.e., 600 and 700°C). The EDCs of the grass chars increased with

289 HTT from 200°C to a maximum at 400°C (0.70 mmol e⁻/g) and decreased with HTT

290 above 400°C. The EDC values of the wood chars were little affected by HTTs

291   between 200 and 400°C and decreased to small values for HTTs≥ 500°C. These

292   trends in EAC and EDC resulted in EEC values that were relatively small for chars

293   formed at low HTTs. EEC values increased with increasing HTT to maximum EEC

294   values at intermediate HTTs of 400 to 500°C to decrease again with increasing HTT>

295   500°C.

296   The absolute EAC and EDC values in **Figure 2a,b** show that both grass and wood

297   chars had a predominance of electron donating (i.e., oxidizable) over electron

298   accepting (i.e., reducible) moieties in low-HTT specimens, while the electron

299   accepting moieties were more abundant than electron donating moieties in high-HTT

300   chars. This effect of HTT becomes more apparent in **Figure 2c,d**, in which the EAC

301   and EDC values are re-plotted as their relative contributions to the total EEC. The

302   EECs were dominated by electron donating moieties in both low-HTT grass and

303   wood chars. Charring at about 400°C led to equal contributions of electron accepting

304   and donating moieties to the EECs. Both char thermosequences showed a similar

305   transition from EDC- to EAC-dominated EECs at HTTs between 300 and 500°C. At

306   HTTs≥ 500°C, the EECs of both grass and wood chars were dominated by the

307   electron accepting moieties. These shifts are consistent with a previous study that

308   reported a decrease in the capacity of sucrose-derived chars to reduce Ag^+ with

309   increasing HTT.[46]

310
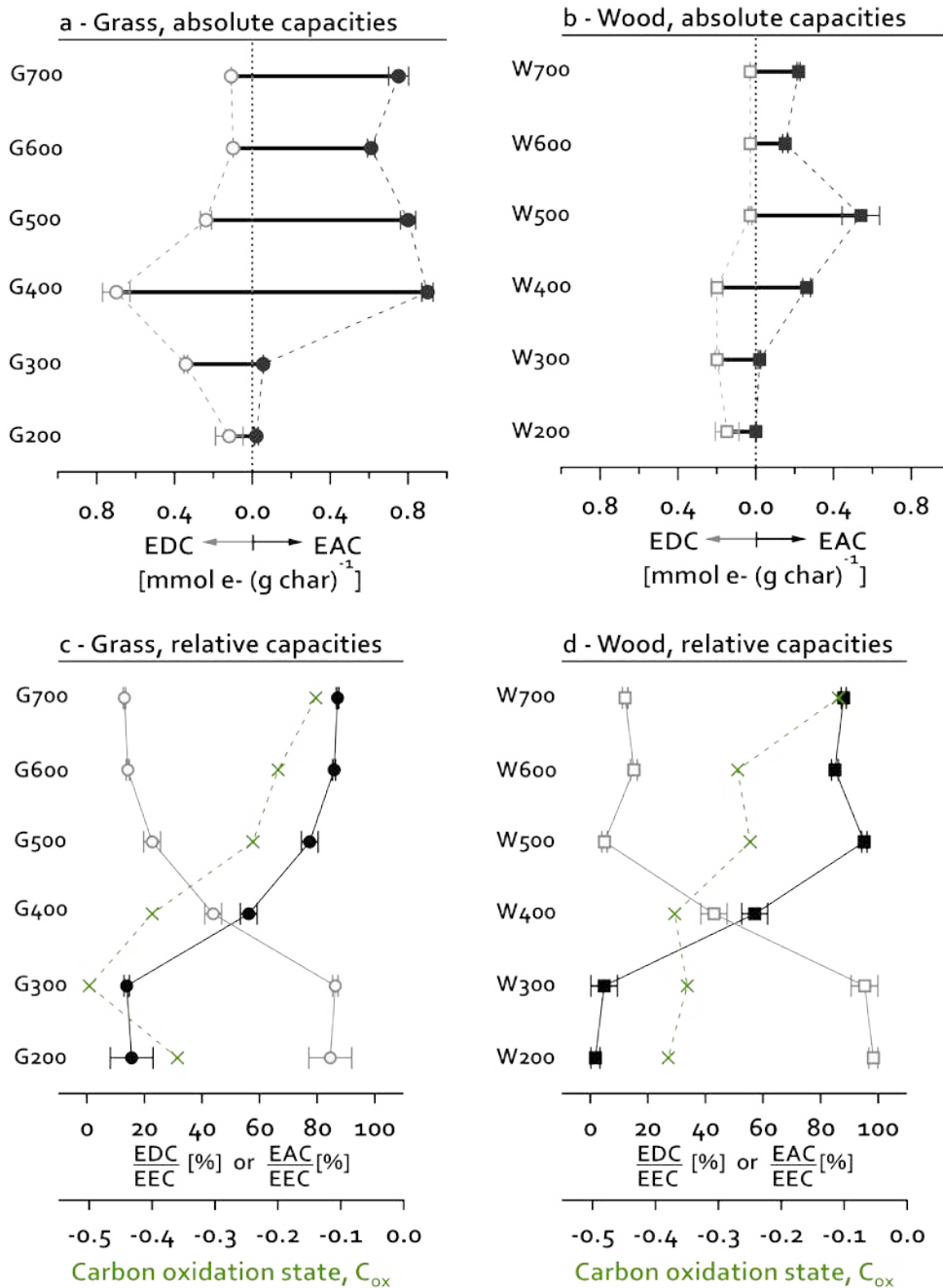
Figure 2. **a,b.** Changes in the electron accepting capacities (EACs) (black solid symbols), electron donating capacities (EDCs) (grey open symbols), and the electron exchange capacities (EECs) (black bars) as a function of the heat treatment temperature (HTT) for the thermosequence chars prepared from grass (GX) and wood (WX), where X denotes the charring temperature in °C. The corresponding carbon-normalized EAC, EDC, and EEC values are provided in the SI. **c,d.** Changes in the relative contributions of EAC and EDC values to the total EEC values as a function of HTT (grey and black lines and symbols) and changes in the average carbon oxidation states, C_{ox}, with HTT (green crosses and dashed lines). Error bars in all panels represent standard deviations from triplicate electrochemical analyses. EAC and EDC values normalized to ash-content corrected char mass and to g C are shown in **Figure S2**.

14

324   ***Effects of charring conditions on char redox properties.*** To assess pyrolysis

325   effects other than HTT on the redox properties of chars, we quantified the EAC and

326   EDC values of an additional six chars formed at HTT of 400/450° C and 700°C and

327   from different feedstock. **Figure S3** shows that the six additional chars also accepted

328   and donated electrons under the used electrochemical conditions, suggesting that the

329   presence of reducible and oxidizable moieties is a common feature of chars. At the

330   same time, chars formed under comparable HTT exhibited a large range in EEC

331   values (i.e., from EEC= 0.34 mmole-/g for DF400 to 2.28 mmole-/g for CW450).

332   RS450 and CW450, which showed the highest EEC values of all tested chars, were

333   both pyrolysed significantly longer (5h for RS450 and CW450) than the other chars

334   tested (e.g., 1h for the thermosequences). **Figure S3** also shows large differences in

335   the EEC values of chars produced at comparable HTT and from similar feedstock but

336   in different pyrolysis systems (e.g., wood as feedstock in CW450 and W450). These

337   findings suggest that factors other than HTT and feedstock have large effects on the

338   redox properties of the chars. These factors may include feedstock processing prior to

339   pyrolysis, the rate and extent of oxygen supply during charring, and the exposure

340   time at a given HTT. [76,77]

341   ***Reversibility of electron transfer to chars.*** We separately assessed the

342   reversibility of electron transfer to the chars by quantifying their changes in EAC and

343   EDC over a borohydride reduction and O_2-reoxidation cycle. We chose BH_4^- as the

344   chemical reductant because it reduces quinones to hydroquinones (i.e., ketones and

345   aldehydes to alcohols),[78,79] it was previously used to reduce electron accepting

346   moieties in carbon blacks[62] and natural organic matter,[80,81] and it is oxidized to

347   borate,[78] which is electro-inactive in the subsequent mediated electrochemical

348   analysis and therefore does not interfere with the EAC and EDC measurements of the

349   chars.

350   The EAC, EDC, and the corresponding EEC values for all untreated, reduced, and

351   re-oxidized chars are provided in **Table S4**. The EEC values of the low-HTT chars

352   (i.e., G200, G300, W200, W300, and W400) increased during the redox cycling. This

353   increase is shown in **Figure 3** as the ratio of the EEC values of the untreated,

354   reduced, and re-oxidized specimen to the (original) EEC of the untreated specimen.

355   The relative increases rather than the absolute increases in EEC are shown in the

356   Figure to aid comparisons among the different chars. The increases in EEC values in

357   the low-HTT chars were mainly caused by an increase in the EDC values (**Table S4**),

358   suggesting that new electron donating moieties were formed. It is possible that the pH

359   increase during BH_4^- treatment resulted in reactions of OH^- with activated aromatic

360   moieties in the chars, leading to the formation of new electron-donating phenolic

361   moieties. However, even though the EEC values of the low-HTT chars increased,

362   they remained smaller than the EEC values of chars formed at HTTs$\geq 400°C$. As

363   compared to the low HTT chars, redox cycling had a much smaller effect on the

364   absolute EEC values of the chars formed at intermediate HTT of 400 to 550 °C

365   (shown for both thermosequences in **Figure 3** and for HZ400, HZ550, DF400,

366   RS450, and CW450 in **Figure S4**). The small changes in the EECs of these chars

367   demonstrate that the chemical reduction and O_2 re-oxidation steps had little effects on

368   the total number of redox-active moieties in these chars. Finally, redox cycling

369   resulted in a decrease in the EEC values of the high HTT-chars (HTT$\geq 600°C$), as

370   shown for G600, G700, W600, and W700 in **Figure 3** and for DF700, and HZ700 in
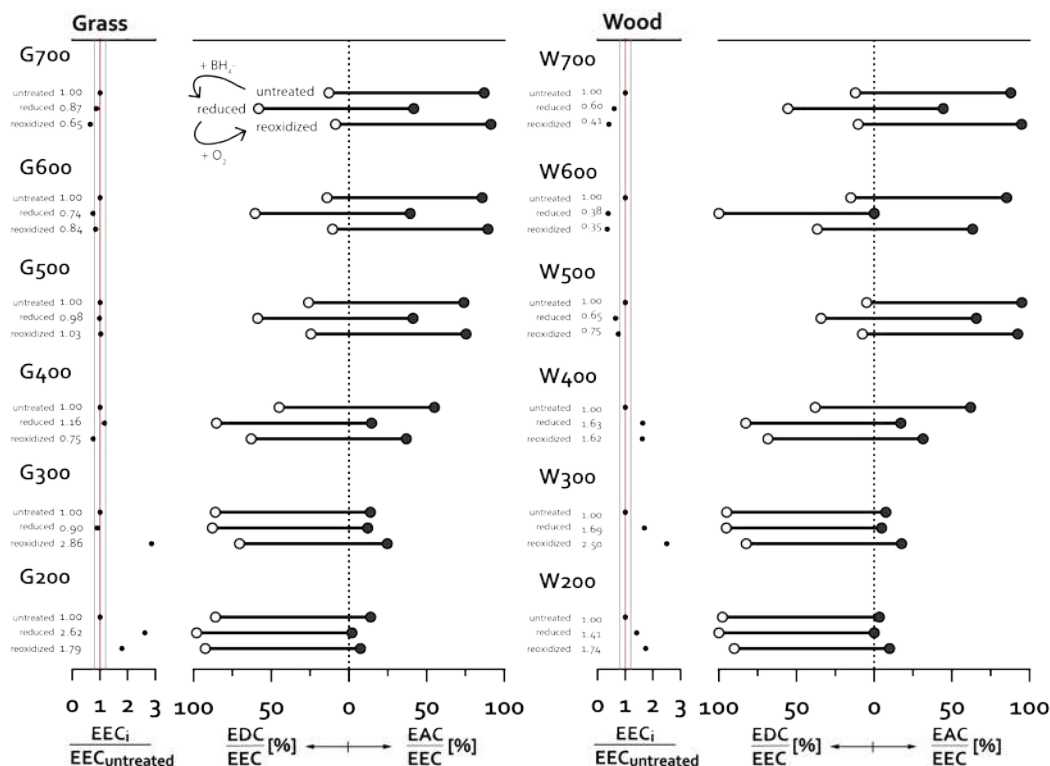
371   **Figure S4**.

Figure 3. Changes in the electron exchange capacities (EECs), electron accepting capacities (EACs) and electron donating capacities (EDCs) of the grass (G) and wood (W) thermosequence chars during redox cycling. Changes in the EECs during redox cycling are expressed relative to the EEC of the untreated chars (i.e., $EEC_i/EEC_{untreated}$ where i corresponds to the untreated, the borohydride (BH_4^-)-reduced and the O_2 re-oxidized char specimen). The $EEC_i/EEC_{untreated}$ values are shown both in numbers and as black dots on the left of each thermosequence. The red line corresponds to $EEC_i/EEC_{untreated}$ of 1, and the outer lines correspond to ratios of 0.8 and 1.2 (i.e., deviations of 20% from the initial EECs). Changes in the relative redox states of the char specimen are expressed as the relative contributions of EAC and EDC values to the total EEC value of each sample (i.e., EAC/EEC and EDC/EEC).

Because redox cycling altered the total number of redox active moieties of some chars, it is difficult to use absolute EAC and EDC values to assess the effects of redox cycling on the redox states of the chars. Changes in the redox states are more apparent when comparing the relative contributions of EAC and EDC to the total EEC value of the untreated, reduced, and re-oxidized chars: the EAC/EEC and EDC/EEC ratios are direct measures of the relative extents of reduction and oxidation of the char specimen, respectively. **Figures 3** and **S4** show that BH_4-treatments

17

393 decreased the EAC/EEC and increased the EDC/EEC ratios of all tested chars,

394 consistent with the reduction of the electron accepting moieties in the chars.

395 Subsequent O_2-exposure of the reduced chars resulted in their re-oxidation, as

396 evidenced by increasing EAC/EEC and decreasing EDC/EEC ratios. The finding that

397 the redox states of all chars responded to changes in the external redox conditions

398 demonstrates that chars may act as redox buffers. Furthermore, electron transfer to

399 and from the intermediate-HTT chars was also largely reversible, as evidenced from

400 only small variations in their EEC values over the reduction and re-oxidation cycle.

401 ***Nature of redox-active moieties in the chars***. In principle, the redox properties of

402 chars may originate from both organic and inorganic constituents. To assess possible

403 contributions of redox active metal species, we quantified Fe and Mn contents in the

404 thermosequence chars by acid digestion and subsequent ICP-OES analysis. The Fe

405 and Mn contents of all thermosequence chars were too small to explain the measured

406 EEC values (**Table S5**). Consequently, organic electron accepting and donating

407 moieties dominated the char redox capacities.

408 There are two possible explanations for the pronounced increase in the EEC values

409 from the low to the intermediate-HTT chars (i.e., 200 & 300°C versus 400 & 500°C):

410 either redox-active organic moieties present in the feedstock (and the low-HTT chars)

411 were accumulated relative to other constituents during charring with increasing HTT

412 or new redox-active moieties were formed in the charring process. We evaluated

413 these two possibilities by relating the changes in EEC values to the respective

414 charring yields (**Table S6**). As detailed in the Supporting Information, this analysis

415 revealed that the EEC increases from low to intermediate-HTT chars were too large

416 to be explained by a relative accumulation of redox active groups. The EEC increases

417 with increasing HTT therefore had to result from neoformation of a large number of

418   electron accepting moieties, which was partly counterbalanced by a decrease in the

419   number of electron donating moieties (as detailed in the Supporting Information).

420   The neoformation of electron accepting moieties is directly supported by an

421   increase in the average carbon oxidation state, C_{ox}, from the low to intermediate-HTT

422   chars that paralleled the increase in the EAC/EEC ratio of these chars (**Figure 2 c,d**).

423   C_{ox} was calculated as

424    $$C_{ox} = \frac{2[O]-[H]-k[N]-m[S]}{[C]} \approx \frac{2[O]-[H]-k[N]}{[C]}$$ **Eq. 2**

425   where [Y] is the content of element Y in the char [mmol Y $(g_{char})^{-1}$] (**Table 1**), and

426   k and m are stoichiometric factors that depend on the oxidation states of N and S in

427   the char.[74] Assuming small sulfur contents, C_{ox} was estimated by the right term in Eq.

428   2. Varying k between the extreme values of +5 and -3 for fully oxidized and reduced

429   N, respectively, resulted in slight changes in the C_{ox} values for the grass but not for

430   the wood thermosequence chars (**Figure S5**). More importantly, however, variations

431   in k did not affect the overall trend of increasing C_{ox} of the chars from both

432   thermosequences with increasing HTT. **Figure 2c,d** shows that the carbon in the low

433   HTT-chars was most reduced (i.e., C_{ox} was most negative with -0.5 and -0.38 for

434   G300 and W200, respectively), consistent with the prevalence of electron donating

435   (i.e., reducing) moieties. We note that C_{ox} for the low HTT-chars was similar to

436   values calculated for lignin (i.e., -0.41, based on published sum formulas for lignin[82]).

437   The intermediate HTT-chars showed a much higher accepting than donating capacity,

438   consistent with the more oxidized carbon (i.e., less negative C_{ox} values) in these

439   chars. C_{ox} values gradually increased with HTT to the highest values of -0.14 and -

440   0.11 for G700 and W700, respectively, and therefore approached $C_{ox}= 0$, the

441   expected value for chars composed of only carbon in condensed aromatic sheets.

442   As detailed in the following, we propose that the pool of redox-active moieties

443   was dominated by electron-donating, phenolic moieties in the low-HTT chars, by

444   newly-formed electron accepting quinone moieties in intermediate-HTT chars, and

445   by electron accepting quinones and possibly condensed aromatics in the high-HTT

446   chars. A plausibility analysis revealed that O was sufficiently abundant in the

447   thermosequence chars to account for the measured EAC and EDC values: assuming

448   that all redox active moieties contained oxygen, as is the case for quinones and

449   phenols, the fraction of O that had to be electroactive ranged between 0.1 - 33% for

450   the EAC and 0.4-6.7% for the EDC of the grass thermosequence chars and between 0

451   - 6% for the EAC and 0.3 - 1.5% for the EDC of the wood thermosequence chars

452   (**Figure S6**).

453   A predominance of phenolic, electron-donating moieties in the low-HTT chars is

454   consistent with these materials being composed of only slightly processed

455   constituents of the feedstock, including lignin, cellulose, and hemicellulose. Lignin is

456   a polyphenolic macromolecule characterized by high EDC and low EAC values, as

457   demonstrated by MER and MEO measurements (**Figure S7**). The redox capacities of

458   lignin agree with the EDC and EAC values in the low-HTT chars. The higher lignin

459   content in wood than grass[83,84] may explain the slightly larger EDC values of W200

460   than G200. We note that cellulose showed only very small current responses in MER

461   and is not electroactive in MEO (**Figure S7**).

462   Intermediate HTT of 400-500°C yield pyrogenic amorphous grass and wood chars

463   which are composed of lignin- and cellulose derived transformation products.[36] While

464   the O contents decrease from low to intermediate-HTT grass and wood chars, the

465   intermediate HTT-chars have higher quinoid C=O contents (**Table 1, Figure 4**).

466   These contents were estimated from C 1s NEXAFS spectra of the thermosequence

467   chars reported in ref. 36, as detailed in the Supporting Information. The higher

468   quinoid C=O contents support quinone moieties as major electron acceptors in the

469   intermediate HTT-chars. A predominance of quinones in these materials is consistent

470   with their reversible electron transfer behavior (**Figure 3**).

471   HTTs of 600 and 700°C further decreased the absolute O contents of the grass and

472   wood chars (**Table 1**). More importantly, the quinoid C=O contents also decreased

473   from intermediate to high HTT. **Figure 4** shows strikingly similar trends of both

474   EAC values and the quinoid C=O contents with HTT: both properties had maxima at

475   intermediate HTTs (around 400 to 500 °C).

476
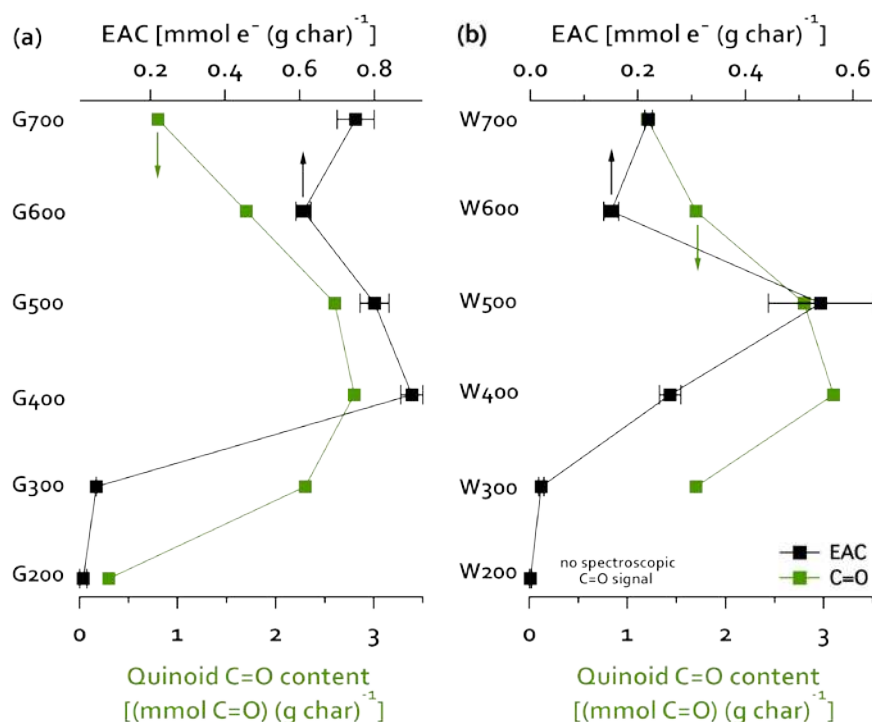
Figure 4. Effect of the heat treatment temperature (HTT) on the estimated quinoid
C=O contents, determined from C=O absorption peaks in C 1s NEXAFS spectra
from reference[36] (green, lower x-axis) and the electron accepting capacities (EACs;
black, upper x-axis) for grass (G; panel a) and wood (W; panel b) thermosequence
chars. Quinoid C=O content and EAC show comparable trends with HTT.

482

483   The ratios of the EAC to the estimated quinoid C=O contents increased with

484   increasing HTT from 0.2 and 0.1 mol e- (mol C=O)$^{-1}$ for G300 and for W300,

485   respectively, to 0.94 and 0.19 mol e- (mol C=O)$^{-1}$ for the G700 and W500

486   thermosequence chars (**Figure S8**). This suggests that quinone moieties were

487   sufficiently abundant to explain the measured EAC values. The combined

488   electrochemical and spectroscopic data therefore strongly support quinones as major

489   electron accepting moieties.

490   The high ratios of EAC to quinoid C=O contents for the high HTT chars (and

491   particularly a ratio of close to unity for G700) may signify an increasing contribution

492   of non-quinoid structures, such as conjugated Π−electron systems, to the EAC with

493   increasing HTT. The formation of polycondensed aromatic structures at high HTT is

494   supported by increasing double bond equivalents, DBE, and the aromaticity index

495   values, AI, from the intermediate to high-HTT chars (**Figure S9**). The DBE and AI

496   values are estimates of char aromaticity and were calculated from the elemental

497   composition data of the chars (Supporting Information). Compared to the DBE, the

498   AI is a more conservative estimate for aromaticity as it accounts for the fact that

499   double bonds of heteroatoms do not necessarily contribute to aromaticity, ring

500   formation or condensation.[75] The high-HTT chars have AI values above the

501   condensation threshold of AI= 0.67, and therefore must contain condensed aromatic

502   structures. Such aromatic clusters were previously reported for a 700°C char.[58]

503

504   **Implications**

505   The results of this work suggest that redox-activity is a general functionality of

506   chars and that chars may be more important as redox-active organic phases in the

507   environment than previously recognized. There are both fundamental biogeochemical

508   and applied engineering implications of this insight. Given that chars are redox

509   active, they are immediate candidates for environmental engineering applications that

510 require or involve controlled and catalytic transfers of electrons. Such applications

511 include reductive pollutant transformations in sediments and the mitigation of nitrous

512 oxide emissions from soils. Of particular interest is the possibility to adjust the

513 electrochemical properties of chars for very specific applications through the choice

514 of pyrolysis conditions (HTT controlling the absolute magnitude of EEC) and

515 feedstock. HTT may be varied to engineer chars that favor either conductance via

516 sheets or redox buffering by quinone/hydroquinone functionalities.

517 The electrochemical properties of chars may further have consequences in a

518 broader biogeochemical context. For example, the presence of char black carbon in

519 many sediments[7,8] raises the question as to whether microbes in these systems can use

520 chars as terminal electron acceptors in anaerobic respiration. A particularly intriguing

521 consequence of our findings pertains to the fundamental question why natural organic

522 matter around the globe is so good at 'shuttling' electrons.[85-87] Our results raise the

523 question whether "humic substances" typically employed as proxies in investigations

524 of electron shuttling phenomena may have developed this capacity not as a result of

525 what used to be called "humification" processes,[88] but because the operational humic

526 extraction procedure includes significant proportions of electrochemically active char

527 components.

528 Our work clearly demonstrates that chars are electroactive in a quantitatively

529 meaningful dimension. This evidence can be combined with the insight that char

530 admixtures are ubiquitous in soil ecosystems worldwide (e.g.,[89-91]). More support for

531 a general contribution of char constituents to the electrochemistry of natural organic

532 matter comes from our observation that the charring temperatures of 400-500°C, that

533 resulted in chars with the highest redox capacities, corresponded to temperatures

534 reported for biomass burning in wildfires.[92,93] Roden et al. [43] used electron energy-

loss spectroscopy to demonstrate that electron shuttling 'solid-phase humic substances' were almost purely aromatic – a molecular property that is hard to rationalize as the result of hypothetical, biotic or abiotic "humification" processes. Admittedly, quinones, phenazines and other electron shuttling moieties may originate from diverse sources. While engineering applications for electrochemically active chars and their residues appear to be obvious, our results also strongly suggest chars may play a larger role in biogeochemically relevant electron transfer reactions than previously recognized.

Associated content

Supporting information. This material is available free of charge via the Internet at http://pubs.acs.org.

Author information

Corresponding author.

Michael Sander

References

1.   Schmidt, M. W. I.; Noack, A. G.; Black carbon in soils and sediments: Analysis, distribution, implications, and current challenges. *Global Biogeochemical Cycles* **2000,** *14*, (3), 777-793.
2.   Dickens, A. F.; Gelinas, Y.; Masiello, C. A.; Wakeham, S.; Hedges, J. I.; Reburial of fossil organic carbon in marine sediments. *Nature* **2004,** *427*, (6972), 336-339.
3.   Kuhlbusch, T. A. J.; Black carbon and the carbon cycle. *Science* **1998,** *280*, (5371), 1903-1904.

564 4. Masiello, C. A.; New directions in black carbon organic geochemistry. *Marine Chemistry* **2004,** *92*, (1-4), 201-213.
566 5. Masiello, C. A.; Druffel, E. R. M.; Black carbon in deep-sea sediments. *Science* **1998,** *280*, (5371), 1911-1913.
568 6. Schmidt, M. W. I.; Biogeochemistry - Carbon budget in the black. *Nature* **2004,** *427*, (6972), 305-+.
570 7. Middelburg, J. J.; Nieuwenhuize, J.; van Breugel, P.; Black carbon in marine sediments. *Marine Chemistry* **1999,** *65*, (3-4), 245-252.
572 8. Gustafsson, O.; Gschwend, P. M.; The flux of black carbon to surface sediments on the New England continental shelf. *Geochimica Et Cosmochimica Acta* **1998,** *62*, (3), 465-472.
575 9. Kuzyakov, Y.; Subbotina, I.; Chen, H. Q.; Bogomolova, I.; Xu, X. L.; Black carbon decomposition and incorporation into soil microbial biomass estimated by C-14 labeling. *Soil Biology & Biochemistry* **2009,** *41*, (2), 210-219.
578 10. Liang, B.; Lehmann, J.; Solomon, D.; Sohi, S.; Thies, J. E.; Skjemstad, J. O.; Luizao, F. J.; Engelhard, M. H.; Neves, E. G.; Wirick, S.; Stability of biomass-derived black carbon in soils. *Geochimica Et Cosmochimica Acta* **2008,** *72*, (24), 6069-6078.
582 11. Skjemstad, J. O.; Taylor, J. A.; Smernik, R. J.; Estimation of charcoal (char) in soils. *Communications in Soil Science and Plant Analysis* **1999,** *30*, (15-16), 2283-2298.
585 12. Sander, M.; Pignatello, J. J.; Characterization of charcoal adsorption sites for aromatic compounds: Insights drawn from single-solute and Bi-solute competitive experiments. *Environmental Science & Technology* **2005,** *39*, (6), 1606-1615.
588 13. Accardi-Dey, A.; Gschwend, P. M.; Reinterpreting literature sorption data considering both absorption into organic carbon and adsorption onto black carbon. *Environmental Science & Technology* **2003,** *37*, (1), 99-106.
591 14. Allen-King, R. M.; Grathwohl, P.; Ball, W. P.; New modeling paradigms for the sorption of hydrophobic organic chemicals to heterogeneous carbonaceous matter in soils, sediments, and rocks. *Advances in Water Resources* **2002,** *25*, (8-12), 985-1016.
595 15. Gustafsson, O.; Haghseta, F.; Chan, C.; MacFarlane, J.; Gschwend, P. M.; Quantification of the dilute sedimentary soot phase: Implications for PAH speciation and bioavailability. *Environmental Science & Technology* **1997,** *31*, (1), 203-209.
598 16. Koelmans, A. A.; Jonker, M. T. O.; Cornelissen, G.; Bucheli, T. D.; Van Noort, P. C. M.; Gustafsson, O.; Black carbon: The reverse of its dark side. *Chemosphere* **2006,** *63*, (3), 365-377.
601 17. Cornelissen, G.; Haftka, J.; Parsons, J.; Gustafsson, O.; Sorption to black carbon of organic compounds with varying polarity and planarity. *Environmental Science & Technology* **2005,** *39*, (10), 3688-3694.
604 18. Cornelissen, G.; Gustafsson, O.; Bucheli, T. D.; Jonker, M. T. O.; Koelmans, A. A.; Van Noort, P. C. M.; Extensive sorption of organic compounds to black carbon, coal, and kerogen in sediments and soils: Mechanisms and consequences for distribution, bioaccumulation, and biodegradation. *Environmental Science & Technology* **2005,** *39*, (18), 6881-6895.
609 19. Beesley, L.; Marmiroli, M.; The immobilisation and retention of soluble arsenic, cadmium and zinc by biochar. *Environmental Pollution* **2011,** *159*, (2), 474-480.

612 20. Uchimiya, M.; Klasson, K. T.; Wartelle, L. H.; Lima, I. M.; Influence of soil
613 properties on heavy metal sequestration by biochar amendment: 1. Copper sorption
614 isotherms and the release of cations. *Chemosphere* **2011,** *82*, (10), 1431-1437.
615 21. Beesley, L.; Moreno-Jimenez, E.; Gomez-Eyles, J. L.; Harris, E.; Robinson,
616 B.; Sizmur, T.; A review of biochars' potential role in the remediation, revegetation
617 and restoration of contaminated soils. *Environmental Pollution* **2011,** *159*, (12),
618 3269-3282.
619 22. Choppala, G. K.; Bolan, N. S.; Megharaj, M.; Chen, Z.; Naidu, R.; The
620 Influence of Biochar and Black Carbon on Reduction and Bioavailability of
621 Chromate in Soils. *Journal of Environmental Quality* **2012,** *41*, (4), 1175-1184.
622 23. Park, J. H.; Choppala, G. K.; Bolan, N. S.; Chung, J. W.; Chuasavathi, T.;
623 Biochar reduces the bioavailability and phytotoxicity of heavy metals. *Plant and Soil*
624 **2011,** *348*, (1-2), 439-451.
625 24. Joseph, S. D.; Camps-Arbestain, M.; Lin, Y.; Munroe, P.; Chia, C. H.; Hook,
626 J.; van Zwieten, L.; Kimber, S.; Cowie, A.; Singh, B. P.; Lehmann, J.; Foidl, N.;
627 Smernik, R. J.; Amonette, J. E.; An investigation into the reactions of biochar in soil.
628 *Australian Journal of Soil Research* **2010,** *48*, (6-7), 501-515.
629 25. Mochidzuki, K.; Soutric, F.; Tadokoro, K.; Antal, M. J.; Toth, M.; Zelei, B.;
630 Varhegyi, G.; Electrical and physical properties of carbonized charcoals. *Industrial &*
631 *Engineering Chemistry Research* **2003,** *42*, (21), 5140-5151.
632 26. Kemper, J. M.; Ammar, E.; Mitch, W. A.; Abiotic degradation of hexahydro-
633 1,3,5-trinitro-1,3,5-triazine in the presence of hydrogen sulfide and black carbon.
634 *Environmental Science & Technology* **2008,** *42*, (6), 2118-2123.
635 27. Xu, W. Q.; Dana, K. E.; Mitch, W. A.; Black Carbon-Mediated Destruction of
636 Nitroglycerin and RDX By Hydrogen Sulfide. *Environmental Science & Technology*
637 **2010,** *44*, (16), 6409-6415.
638 28. Yu, X. D.; Gong, W. W.; Liu, X. H.; Shi, L.; Han, X.; Bao, H. Y.; The use of
639 carbon black to catalyze the reduction of nitrobenzenes by sulfides. *Journal of*
640 *Hazardous Materials* **2011,** *198*, 340-346.
641 29. Oh, S. Y.; Son, J. G.; Lim, O. T.; Chiu, P. C.; The role of black carbon as a
642 catalyst for environmental redox transformation. *Environmental Geochemistry and*
643 *Health* **2012,** *34*, 105-113.
644 30. Oh, S. Y.; Son, J. G.; Chiu, P. C.; Biochar-mediated reductive transformation
645 of nitro herbicides and explosives. *Environmental Toxicology and Chemistry* **2013,**
646 *32*, (3), 501-508.
647 31. Oh, S. Y.; Son, J. G.; Hur, S. H.; Chung, J. S.; Chiu, P. C.; Black Carbon-
648 Mediated Reduction of 2,4-Dinitrotoluene by Dithiothreitol. *Journal of*
649 *Environmental Quality* **2013,** *42*, (3), 815-821.
650 32. Xu, W. Q.; Pignatello, J. J.; Mitch, W. A.; Role of Black Carbon Electrical
651 Conductivity in Mediating Hexahydro-1,3,5-trinitro-1,3,5-triazine (RDX)
652 Transformation on Carbon Surfaces by Sulfides. *Environmental Science &*
653 *Technology* **2013,** *47*, (13), 7129-7136.
654 33. Cayuela, M. L.; Sanchez-Monedero, M. A.; Roig, A.; Hanley, K.; Enders, A.;
655 Lehmann, J.; Biochar and denitrification in soils: when, how much and why does
656 biochar reduce N2O emissions? *Scientific Reports* **2013,** *3*.
657 34. Harter, J.; Krause, H.-M.; Schuettler, S.; Ruser, R.; Fromme, M.; Scholten, T.;
658 Kappler, A.; Behrens, S.; Linking N2O emissions from biochar-amended soil to the
659 structure and function of the N-cycling microbial community. *The ISME Journal*
660 **2013**, 1-15.

661 35. Cayuela, M. L.; van Zwieten, L.; Singh, B. P.; Jeffery, S.; Roig, A.; Sánchez-
662 Monedero, M. A.; Biochar's role in mitigating soil nitrous oxide emissions: A review
663 and meta-analysis. *Agriculture, Ecosystems and Environment* **2013**.
664 36. Keiluweit, M.; Nico, P. S.; Johnson, M. G.; Kleber, M.; Dynamic molecular
665 structure of plant biomass-derived black carbon (biochar). *Environmental Science &*
666 *Technology* **2010,** *44*, (4), 1247-1253.
667 37. Heymann, K.; Lehmann, J.; Solomon, D.; Schmidt, M. W. I.; Regier, T.; C 1s
668 K-edge near edge X-ray absorption fine structure (NEXAFS) spectroscopy for
669 characterizing functional group chemistry of black carbon. *Organic Geochemistry*
670 **2011,** *42*, (9), 1055-1064.
671 38. Emmerich, F. G.; Rettori, C.; Luengo, C. A.; ESR in heat treated carbons
672 from the endocarp of babassu coconut. *Carbon* **1991,** *29*, (3), 305-311.
673 39. Scott, D. T.; McKnight, D. M.; Blunt-Harris, E. L.; Kolesar, S. E.; Lovley, D.
674 R.; Quinone moieties act as electron acceptors in the reduction of humic substances
675 by humics-reducing microorganisms. *Environmental Science & Technology* **1998,** *32*,
676 (19), 2984-2989.
677 40. Aeschbacher, M.; Sander, M.; Schwarzenbach, R. P.; Novel electrochemical
678 approach to assess the redox properties of humic substances. *Environmental Science*
679 *& Technology* **2010,** *44*, (1), 87-93.
680 41. Aeschbacher, M.; Vergari, D.; Schwarzenbach, R. P.; Sander, M.;
681 Electrochemical Analysis of Proton and Electron Transfer Equilibria of the Reducible
682 Moieties in Humic Acids. *Environmental Science & Technology* **2011,** *45*, (19),
683 8385-8394.
684 42. Dunnivant, F. M.; Schwarzenbach, R. P.; Macalady, D. L.; Reduction of
685 substituted nitrobenzenes in aqueous solutions containing natural organic matter.
686 *Environmental Science & Technology* **1992,** *26*, (11), 2133-2141.
687 43. Roden, E. E.; Kappler, A.; Bauer, I.; Jiang, J.; Paul, A.; Stoesser, R.; Konishi,
688 H.; Xu, H. F.; Extracellular electron transfer through microbial reduction of solid-
689 phase humic substances. *Nature Geoscience* **2010,** *3*, (6), 417-421.
690 44. Zhang, C. F.; Katayama, A.; Humin as an Electron Mediator for Microbial
691 Reductive Dehalogenation. *Environmental Science & Technology* **2012,** *46*, (12),
692 6575-6583.
693 45. Matsumura, Y.; Hagiwara, S.; Takahashi, H.; Automated potentiometric
694 titration of surface acidity of carbon black. *Carbon* **1976,** *14*, (3), 163-167.
695 46. Garten, V. A.; Weiss, D. E.; The quinone-hydroquinone character of activated
696 carbon and carbon black. *Australian Journal of Chemistry* **1955,** *8*, (1), 68-95.
697 47. Tarasevich, M. R.; Bogdanovskaya, V. A.; Zagudaeva, N. M.; Redox
698 reactions of quinones on carbon materials. *Journal of Electroanalytical Chemistry*
699 **1987,** *223*, (1-2), 161-169.
700 48. Studebaker, M. L.; Huffman, E. W. D.; Wolfe, A. C.; Nabors, L. G.; Oxygen-
701 containing groups on the surface of carbon black. *Industrial and Engineering*
702 *Chemistry* **1956,** *48*, (1), 162-166.
703 49. Langley, L. A.; Fairbrother, D. H.; Effect of wet chemical treatments on the
704 distribution of surface oxides on carbonaceous materials. *Carbon* **2007,** *45*, (1), 47-
705 54.
706 50. Kongkanand, A.; Kamat, P. V.; Interactions of single wall carbon nanotubes
707 with methyl viologen radicals. Quantitative estimation of stored electrons. *Journal of*
708 *Physical Chemistry C* **2007,** *111*, (26), 9012-9015.

709 51.   Kongkanand, A.; Kamat, P. V.; Electron storage in single wall carbon
710 nanotubes. Fermi level equilibration in semiconductor-SWCNT suspensions. *Acs*
711 *Nano* **2007,** *1*, (1), 13-21.
712 52.   Xie, Q. S.; Perezcordero, E.; Echegoyen, L.; Electrochemical detection of
713 C606- and C706- - Enhanced stability of fullerides in solution. *Journal of the*
714 *American Chemical Society* **1992,** *114*, (10), 3978-3980.
715 53.   Dubois, D.; Kadish, K. M.; Flanagan, S.; Wilson, L. J.; Electrochemical
716 detection of fulleronium and highly reduced fulleride (C60(5-)) ions in solution.
717 *Journal of the American Chemical Society* **1991,** *113*, (20), 7773-7774.
718 54.   Krishnamurthy, S.; Lightcap, I. V.; Kamat, P. V.; Electron transfer between
719 methyl viologen radicals and graphene oxide: Reduction, electron storage and
720 discharge. *Journal of Photochemistry and Photobiology a-Chemistry* **2011,** *221*, (2-
721 3), 214-219.
722 55.   Lightcap, I. V.; Kosel, T. H.; Kamat, P. V.; Anchoring Semiconductor and
723 Metal Nanoparticles on a Two-Dimensional Catalyst Mat. Storing and Shuttling
724 Electrons with Reduced Graphene Oxide. *Nano Letters* **2010,** *10*, (2), 577-583.
725 56.   McBeath, A. V.; Smernik, R. J.; Variation in the degree of aromatic
726 condensation of chars. *Organic Geochemistry* **2009,** *40*, (12), 1161-1168.
727 57.   McBeath, A. V.; Smernik, R. J.; Schneider, M. P. W.; Schmidt, M. W. I.;
728 Plant, E. L.; Determination of the aromaticity and the degree of aromatic
729 condensation of a thermosequence of wood charcoal using NMR. *Organic*
730 *Geochemistry* **2011,** *42*, (10), 1194-1202.
731 58.   Cao, X. Y.; Pignatello, J. J.; Li, Y.; Lattao, C.; Chappell, M. A.; Chen, N.;
732 Miller, L. F.; Mao, J. D.; Characterization of Wood Chars Produced at Different
733 Temperatures Using Advanced Solid-State C-13 NMR Spectroscopic Techniques.
734 *Energy & Fuels* **2012,** *26*, (9), 5983-5991.
735 59.   Nishimiya, K.; Hata, T.; Imamura, Y.; Ishihara, S.; Analysis of chemical
736 structure of wood charcoal by X-ray photoelectron spectroscopy. *Journal of Wood*
737 *Science* **1998,** *44*, (1), 56-61.
738 60.   Rhim, Y.-R.; Zhang, D.; Fairbrother, D. H.; Wepasnick, K. A.; Livi, K. J.;
739 Bodnar, R. J.; Nagle, D. C.; Changes in electrical and microstructural properties of
740 microcrystalline cellulose as function of carbonization temperature. *Carbon* **2010,** *48*,
741 (4), 1012-1024.
742 61.   Bauer, M.; Heitmann, T.; Macalady, D. L.; Blodau, C.; Electron transfer
743 capacities and reaction kinetics of peat dissolved organic matter. *Environmental*
744 *Science & Technology* **2007,** *41*, (1), 139-145.
745 62.   Matsumura, Y.; Takahashi, H.; Potentiometric redox titration of quinone in
746 carbon black with NaBH4 and I2. *Carbon* **1979,** *17*, (2), 109-114.
747 63.   Peretyazhko, T.; Sposito, G.; Reducing capacity of terrestrial humic acids.
748 *Geoderma* **2006,** *137*, (1-2), 140-146.
749 64.   Struyk, Z.; Sposito, G.; Redox properties of standard humic acids. *Geoderma*
750 **2001,** *102*, (3-4), 329-346.
751 65.   Graber, E. R.; Tschansky, L.; Cohen, E.; Reducing capacity of water extracts
752 of biochars and their solubilization of soil Mn and Fe. *European Journal of Soil*
753 *Science* **2013,** *asap*.
754 66.   Aeschbacher, M.; Graf, C.; Schwarzenbach, R. P.; Sander, M.; Antioxidant
755 Properties of Humic Substances. *Environmental Science & Technology* **2012,** *46*, (9),
756 4916-4925.
757 67.   Gorski, C. A.; Aeschbacher, M.; Soltermann, D.; Voegelin, A.; Baeyens, B.;
758 Fernandes, M. M.; Hofstetter, T. B.; Sander, M.; Redox Properties of Structural Fe in

Clay Minerals. 1. Electrochemical Quantification of Electron-Donating and - Accepting Capacities of Smectites. *Environmental Science & Technology* **2012,** *46*, (17), 9360-9368.

68.   Gorski, C. A.; Klupfel, L.; Voegelin, A.; Sander, M.; Hofstetter, T. B.; Redox Properties of Structural Fe in Clay Minerals. 2. Electrochemical and Spectroscopic Characterization of Electron Transfer Irreversibility in Ferruginous Smectite, SWa-1. *Environmental Science & Technology* **2012,** *46*, (17), 9369-9377.

69.   Gorski, C. A.; Kluepfel, L.; Voegelin, A.; Sander, M.; Hofstetter, T. B.; Redox properties of structural Fe in clay minerals: 3. Relationships between smectite redox and structural properties. *Environmental Science & Technology* **2013,** *47*, (23), 13477-13485.

70.   Fulton, W.; Gray, M.; Prahl, F.; Kleber, M.; A simple technique to eliminate ethylene emissions from biochar amendment in agriculture. *Agronomy for Sustainable Development* **2013,** *33*, (3), 469-474.

71.   Kaal, J.; Schneider, M. P. W.; Schmidt, M. W. I.; Rapid molecular screening of black carbon (biochar) thermosequences obtained from chestnut wood and rice straw: A pyrolysis-GC/MS study. *Biomass and Bioenergy* **2012,** *45*, (C), 115-129.

72.   Hammes, K.; Smernik, R. J.; Skjemstad, J. O.; Herzog, A.; Vogt, U. F.; Schmidt, M. W. I.; Synthesis and characterisation of laboratory-charred grass straw (Oryza saliva) and chestnut wood (Castanea sativa) as reference materials for black carbon quantification. *Organic Geochemistry* **2006,** *37*, (11), 1629-1633.

73.   Hammes, K.; Smernik, R. J.; Skjemstad, J. O.; Schmidt, M. W. I.; Characterisation and evaluation of reference materials for black carbon analysis using elemental composition, colour, BET surface area and C-13 NMR spectroscopy. *Applied Geochemistry* **2008,** *23*, (8), 2113-2122.

74.   Masiello, C. A.; Gallagher, M. E.; Randerson, J. T.; Deco, R. M.; Chadwick, O. A.; Evaluating two experimental approaches for measuring ecosystem carbon oxidation state and oxidative ratio. *Journal of Geophysical Research* **2008,** *113*, (G3), G03010.

75.   Koch, B. P.; Dittmar, T.; From mass to structure: an aromaticity index for high-resolution mass data of natural organic matter. *Rapid Commun. Mass Spectrom.* **2006,** *20*, (5), 926-932.

76.   Soucemarianadin, L. N.; Quideau, S. A.; MacKenzie, M. D.; Bernard, G. M.; Wasylishen, R. E.; Laboratory charring conditions affect black carbon properties: A case study from Quebec black spruce forests. *Organic Geochemistry* **2013,** *62*, 46-55.

77.   Cantrell, K. B.; Hunt, P. G.; Uchimiya, M.; Novak, J. M.; Ro, K. S.; Impact of pyrolysis temperature and manure source on physicochemical characteristics of biochar. *Bioresource Technology* **2012,** *107*, 419-428.

78.   Chaikin, S. W.; Brown, W. G.; Reduction of aldehydes, ketones and acid chlorides by sodium borohydride. *Journal of the American Chemical Society* **1949,** *71*, (1), 122-125.

79.   Johnson, M. R.; Rickborn, B.; Sodium borohydride reduction of conjugated aldehydes and ketones. *Journal of Organic Chemistry* **1970,** *35*, (4), 1041-&.

80.   Ma, J. H.; Del Vecchio, R.; Golanoski, K. S.; Boyle, E. S.; Blough, N. V.; Optical Properties of Humic Substances and CDOM: Effects of Borohydride Reduction. *Environmental Science & Technology* **2010,** *44*, (14), 5395-5402.

81.   Thorn, K. A.; Pettigrew, P. J.; Goldenberg, W. S.; Covalent binding of aniline to humic substances .2. N-15 NMR studies of nucleophilic addition reactions. *Environmental Science & Technology* **1996,** *30*, (9), 2764-2775.

808 82. Adler, E.; Lignin chemistry—past, present and future. *Wood Science and*
809 *Technology* **1977,** *11*, (3), 169-218.
810 83. Demirbaş, A.; Relationships between lignin contents and heating values of
811 biomass. *Energy conversion and management* **2001,** *42*, (2), 183-188.
812 84. Fahmi, R.; Bridgwater, A. V.; Darvell, L. I.; Jones, J. M.; Yates, N.; Thain, S.;
813 Donnison, I. S.; The effect of alkali metals on combustion and pyrolysis of Lolium
814 and Festuca grasses, switchgrass and willow. *Fuel* **2007,** *86*, (10-11), 1560-1569.
815 85. Lovley, D. R.; Coates, J. D.; BluntHarris, E. L.; Phillips, E. J. P.; Woodward,
816 J. C.; Humic substances as electron acceptors for microbial respiration. *Nature* **1996,**
817 *382*, (6590), 445-448.
818 86. Sposito, G., Electron Shuttling by Natural Organic Matter: Twenty Years
819 After. In *Aquatic Redox Chemistry*, Tratnyek, P. G.; Grundl, T. J.; Haderlein, S. B.,
820 Eds. 2011; Vol. 1071, pp 113-127.
821 87. Kluepfel, L.; Piepenbrock, A.; Kappler, A.; Sander, M.; Humic substances as
822 fully regenerable electron acceptors in recurrently anoxic environments. *Nature*
823 *Geoscience* **2014,** *accepted*.
824 88. Essington, M. E., *Soil and Water Chemistry: An Integrative Approach*. CRC
825 Press: 2003.
826 89. Skjemstad, J. O.; Reicosky, D. C.; Wilts, A. R.; McGowan, J. A.; Charcoal
827 carbon in US agricultural soils. *Soil Science Society of America Journal* **2002,** *66*, (4),
828 1249-1255.
829 90. Ohlson, M.; Dahlberg, B.; Okland, T.; Brown, K. J.; Halvorsen, R.; The
830 charcoal carbon pool in boreal forest soils. *Nature Geoscience* **2009,** *2*, (10), 692-695.
831 91. Rodionov, A.; Amelung, W.; Peinemann, N.; Haumaier, L.; Zhang, X. D.;
832 Kleber, M.; Glaser, B.; Urusevskaya, I.; Zech, W.; Black carbon in grassland
833 ecosystems of the world. *Global Biogeochemical Cycles* **2010,** *24*.
834 92. Alexis, M. A.; Rasse, D. P.; Rumpel, C.; Bardoux, G.; Péchot, N.; Schmalzer,
835 P.; Drake, B.; Mariotti, A.; Fire impact on C and N losses and charcoal production in
836 a scrub oak ecosystem. *Biogeochemistry* **2007,** *82*, (2), 201-216.
837 93. Gimeno-Garcia, E.; Andreu, V.; Rubio, J. L.; Spatial patterns of soil
838 temperatures during experimental fires. *Geoderma* **2003,** *118*, (1-2), 17-38.
839